GRAVITATIONAL SIGNATURES OF LUNAR FLOOR FRACTURED CRATERS Thorey clément, Chloé Michaut and Mark Wieczorek , Université Paris Diderot, Sorbonne Paris Cité, Institut de Physique du Globe de Paris, F-75013 Paris, France, thorey@ipgp.fr

Introduction: About 200 Floor Fractured Craters (FFCs) have been identified by [1] on the Moon. These craters are characterized by distinctive shallow floors and numerous floor fractures that suggest an endogenous process of modification. Intrusion of magma beneath the crater floor and viscous relaxation of the crater topography after the impact are two proposed scenarios to explain these deformations.

Our recent theoretical model for the dynamics of crater-centered intrusions [2] and morphological and geological studies [3] showed that intrusion of magma beneath the crater floor is the most reliable scenario to produce the morphological features observed at FFCs. Magmatic intrusions should be emplaced at their level of neutral buoyancy. Upon cooling and solidification, however, their densities will be larger than the surrounding crustal material and hence leave a positive signature in the gravity field. Guided by the predictions of our theoretical model [2], we investigate here the potential gravitational signatures of crater-centered intrusions on the Moon. We compare them with the gravity field recorded by the Gravity Recovery and Interior Laboratory (GRAIL) [4] at the sites of FFCs in order to obtain insights into magma transport and physical properties.

Theoretical considerations: The Bouguer anomaly associated with a magmatic intrusion beneath a crater depends upon the intrusion characteristics. Recently, we showed that the morphology of crater-centered intrusions depends upon the overlying layer properties, in particular the thickness of the overlying elastic layer [2]. For an overlying layer with no elastic strength or an elastic layer sufficiently thin compared to the crater size, the intrusion is predicted to be flat and close to cylindrical; the crater floor shows a plate-like topography (Figure 1, top left). On the contrary, when the intrusion is emplaced beneath a thick elastic layer relatively to the crater size, the intrusions is bell-shaped and the crater floor appears convex (Figure 1: top right). Accordingly, the classification based on six categories proposed by [1] can be simplified into two main FFC types when considering their gravitational signals: flat floor (class 3, 5 and 6) and convex floor (class 2 and 4) FFCs.

The bottom panel of Figure 1 shows the synthetic Bouguer anomaly expected in both cases for a 100 km diameter crater. For these models, a large, 2 km thick, crater-centered intrusion is emplaced with density contrast of 500 kg m^{-3}. These are the maximum expected values for these parameters, and gives rise to the maximum expected gravity anomaly. The two intrusion shapes result in two different types of anomaly. For a flat-top cylindrical intrusion, i.e. a flat floor FFC, the anomaly is about 44 mGal; it is uniform over the entire crater floor and sharply decreases at the crater rim. In contrast, for a bell-shaped intrusion, i.e. a convex floor FFC, the expected anomaly is smaller in amplitude by 8 mGal and the shape of the gravity anomaly is also bell-shaped. The gravity anomaly for convex floor FFCs should therefore be harder to detect.

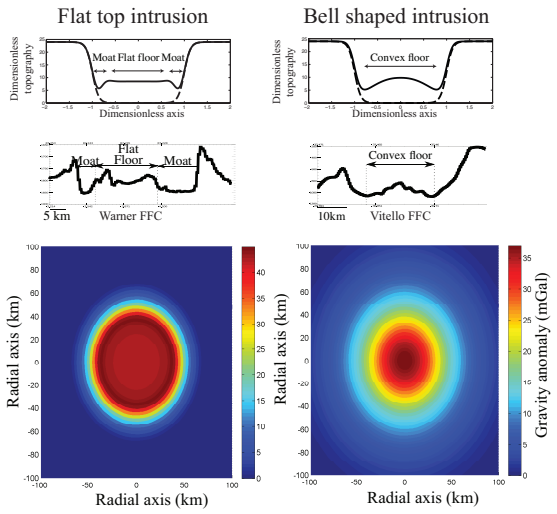

Figure 1: (Top left) 1D profile showing the initial (dashed line) and final (solid line) modeled floor topography for an intrusion that is emplaced at a shallow depth below the crater floor. (Top right) same plot, but for an intrusion that is emplaced deeper below the surface. (Middle left) Floor fractured crater Warner, a 35 km diameter crater that shows a shallowed flat floor. (Middle right) Floor fractured crater Briggs, a 37 km diameter crater that shows a shallowed convex floor. (Bottom left) Synthetic Bouguer anomaly produced by a 100 km diameter and 2 km thick cylinder-like intrusion. (Bottom right) Same plot, but for a convex-like intrusion.

Procedure: The gravity field provided by the Gravity Recovery and Interior Laboratory (GRAIL) mission, used in combination with the topographic dataset obtained from the Lunar Orbiter Laser Altimeter (LOLA) instrument allows to investigate mass anomalies located in the lunar crust. We made use of the primary mission spherical harmonic degree 660 field of [5], and using the crustal model of [6], we removed the gravitational contribution of surface topography, long wavelength lateral variations in crustal density, and lateral variations in crustal thickness. The remaining signal represents short wavelength variations in density of the upper crust.

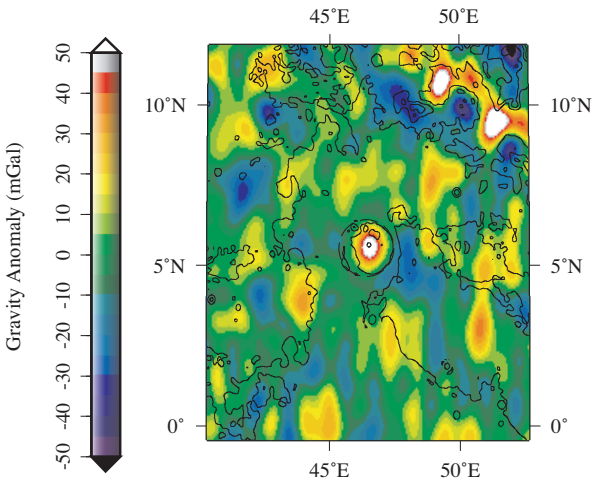

Figure 2: Gravity anomaly of an area centered around the floor fractured crater Taruntius (5.0°N,46.3°E) after removing the contributions of surface topography, crustal variations, and large scale lateral variations in crustal density [6]. The black dashed line represents the crater rim. A positive gravity anomaly with a mean value of 41 mGals is found in the central position of the crater.

To minimize shortwavelength noise, the spherical harmonic coefficients were cosine tapered between degrees 350 and 450 (as an example, see Figure 2 for the floor fractured crater Taruntius).

We used the dataset obtained by [3] as a reference catalog for FFCs. Large impact basins on the nearside of the Moon are filled with thick basaltic lava flows that might have masked the signal from possible magmatic intrusions of the same density. For this reason, we discarded all the floor fractured craters that lie within the lunar maria. Furthermore, filtering the gravity map produced important artifacts around the large mascon basins; therefore, we also removed craters adjacent to the mascon basins. In the end, we worked with a population of 68 floor fractured craters with diameters between 20 and 100 km. For comparison, we also picked 5 different populations of 68 craters from the farside highlands, that showed no evidence for post impact deformations, with the same size-frequency distribution as the floor fractured craters.

For each crater, we defined the gravity anomaly as the mean value of the measured gravity anomaly within the crater's topographic rim and we looked at the correlation between this anomaly and the crater topography.

Results and discussion: Histograms of the gravity anomaly for the FFCs and normal highland craters are shown in Figure 3. The mean anomaly of the FFCs is positive and is equal to 5.3 mGals, whereas the mean of the normal craters is slightly negative and equal to -2.0 mGals. Within the FFCs population, 61% show a flat floor with a mean anomaly of 6.2 mGal. In contrast, 31% show a convex floor with a mean anomaly of 3.9 mGal (Figure 3: right)

As a group, floor fractured craters have positive gravity anomalies that are consistent with our model of crustal intrusions. The average difference between FFCs and normal highland craters is 7 mGal which, for a density contrast of 500 km m^{-3}, corresponds to an average intrusion thickness of 400 m. Nevertheless, the similarity in the distribution of normal and floor fractured craters suggest that the natural variations in gravity signals of impact craters might overwhelm the signal generated by subcrustal intrusions for some FFCs. An analysis of the morphology of crater gravity signals may be capable of distinguishing the signal of magmatic intrusions from other processes.

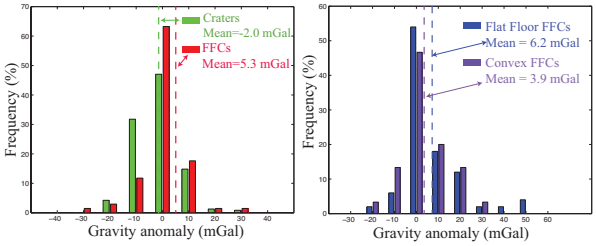

Figure 3: (Left) distribution of the average gravity anomaly above the crater floor for the whole population of FFCs and an average of 5 similarly sized normal crater populations in the highlands. (Right) distributions for the two main morphologies of FFCs, flat and convex floors. Vertical dashed lines correspond to the mean values of each crater population.

References: [1] Schultz (1976), *The Moon*, *15*(3-4). [2] Thorey et al (2013), *JGR*, *In press*. [3] Jozwiak et al (2012), *JGR: Planets*, *117*(E11). [4] Zuber et al (2013), *Science*, *339*(E339). [5] Konopliv et al (2013), *JGR*, *118*(E7) [6] Wieczorek et al (2013), *Science*, *339*(6120). [7] Head et al (2010), *Science*, *329*(5998).